The Plant Cell, Vol. 7, 2001-2011, December 1995

Control of Flower Development and Phyllotaxy by Meristem Identity Genes in Antirrhinum

Rosemary Carpenter,[1] Lucy Copsey, Coral Vincent, Sandra Doyle, Ruth Magrath, and Enrico Coen

Genetics Department, John Innes Centre, Colney Lane, Norwich NR4 7UH, United Kingdom

The flower meristem identity genes *floricaula* (*flo*) and *squamosa* (*squa*) promote a change in phyllotaxy from spiral to whorled in Antirrhinum. To determine how this might be achieved, we have performed a combination of morphological, genetic, and expression analyses. Comparison of the phenotypes and RNA expression patterns of single and double mutants with the wild type showed that *flo* and *squa* act together to promote flower development but that *flo* is epistatic to *squa* with respect to early effects on phyllotaxy. We propose that a common process underlies the phyllotaxy of wild-type, *flo*, and *squa* meristem development but that the relative timing of primordium initiation or growth is altered. This process depends on two separable events: setting aside zones for potential primordium initiation and partitioning these zones into discrete primordia. Failure of the second event can lead to the formation of continuous double spirals, which are occasionally seen in *flo* mutants.

INTRODUCTION

The arrangement of organs around the axis of growth, termed phyllotaxy, is a key feature of plant growth. In one type of arrangement, each node of the stem bears a single organ, set at a fixed angle relative to organs at the nodes above and below it. This results in either spiral phyllotaxy or, if the angle is 180°, an alternating arrangement of organs on opposite sides of the stem, termed opposite or distichous phyllotaxy. In another type of arrangement, whorled phyllotaxy, two or more organs are produced at each node. In many plant species, phyllotaxy is under developmental control, with several patterns of organ arrangement being displayed during different phases of growth. This reflects developmental variation in the properties of meristems, groups of dividing cells that produce organ primordia on their periphery. The pattern with which primordia are set aside or partitioned from the meristem determines the final arrangement of organs around the axis of growth. There have been many attempts to explain how different types of phyllotaxy might arise (e.g., Mitchison, 1977; Richter and Schranner, 1978; Marc and Hackett, 1991; Green, 1992; Callos and Medford, 1994), but there have been few studies on how changes in phyllotaxy might be genetically controlled. Several mutants that alter phyllotaxy in clearly defined ways have been described. For example, one class of mutation changes the behavior of meristems from producing organs in a whorled phyllotaxy to producing them in a spiral phyllotaxy (Coen et al., 1990; Schultz and Haughn, 1991; Huijser et al., 1992; Weigel et al., 1992). To determine how genes might interact to control this switch in the properties of meristems, we analyzed the interactions between two such mutants, *floricaula* (*flo*) and *squamosa* (*squa*), that affect phyllotaxy in Antirrhinum.

Wild-type Antirrhinum exhibits three major types of phyllotaxy during its growth. During early vegetative growth, a whorl of two leaves is produced at each node, with successive leaf pairs being set at right angles to each other (decussate phyllotaxy). When the plant enters the reproductive phase of growth, it switches to spiral phyllotaxy, producing single small leaflike organs, bracts, at each node along the main stem. A flower arises in the axil of each bract (i.e., in the angle between the bract and the main stem) and produces four different types of organs in a whorled phyllotaxy: five sepals, five petals, five stamens (the uppermost stamen fails to develop fully), and two carpels. This whorled arrangement depends on the action of two meristem identity genes, *flo* and *squa*, both of which are expressed in very young floral meristems (Coen et al., 1990; Huijser et al., 1992). If either of these genes is inactivated by a mutation, flowers are replaced by shoots bearing bracts or bracteoles in a near-spiral rather than whorled arrangement.

To understand how *flo* and *squa* might interact to promote the switch in phyllotaxy from spiral to whorled, we performed a combination of morphological, genetic, and expression analyses. Comparison of the phenotypes and RNA expression patterns of single and double mutants with the wild type shows that *flo* and *squa* act together to promote flower development, but *flo* is epistatic to *squa* with respect to early effects on phyllotaxy. We propose that a common process underlies the phyllotaxy of wild-type, *flo*, and *squa* meristem development, but in each case, the relative timing of primordium initiation or growth is altered. This process depends on two separable events: setting aside zones for potential primordium initiation

[1] To whom correspondence should be addressed.

and partitioning these zones into discrete primordia. Failure of the second event can lead to the formation of continuous double spirals, which are occasionally seen in *flo* mutants.

RESULTS

Early Flower Development in the Wild Type

The inflorescence of wild-type Antirrhinum comprises a spiral arrangement of flowers, with the oldest flowers at the base and the youngest at the top of the inflorescence. Flowers and their subtending bracts (nodes) are numbered sequentially starting from the top of the inflorescence. There are ~50 to 60 nodes from the apex to the first fully opened flower. Two axes that bisect each flower can be defined. The dorsoventral (DV) axis extends vertically through each flower. At right angles to this axis lies the mediolateral (ML) axis that runs horizontally.

The morphology of flowers at different stages of development was determined using scanning electron microscopy on plastic replicas of inflorescence apices (Green and Linstead, 1990). Several apices were used for each genotype. Because the developmental stage of a meristem at a given node may depend on genetic background, stock JI 98 was used as a standard wild type. Many of the mutants analyzed were derived by self-pollination from this stock and therefore share a similar genetic background (i.e., *flo-613*, *flo-640*, and *squa-641*). We describe floral development up to approximately node 18 in detail and divide it into six stages: (0) bract mound and tongue, (1) eye, (2) loaf, (3) pentagon, (4) floritypic, and (5) petal mound. These stages are comparable to those in Arabidopsis, with the exception of stage 0, because Arabidopsis lacks bracts (Smyth et al., 1990). Approximate sizes of the floral meristems or cells, indicated in brackets (ML and DV), were measured in micrometers along the different axes.

Stage 0: Bract Tongue (Nodes 0 to 4)

The inflorescence apex had a central region of ~15 cells in diameter, the apical zone, in which no primordia were visible. The first visible node was a small mound of ~4 or 5 cells in diameter lying on the periphery of the apical zone (Figure 1). The cells of both the apical zone and the mound were approximately isodiametric in shape and 8 to 10 μm across. By approximately node 1 or 2, tongue-shaped bract primordia were visible, each separated by a crease from the inflorescence apex. When first seen, the crease was approximately seven

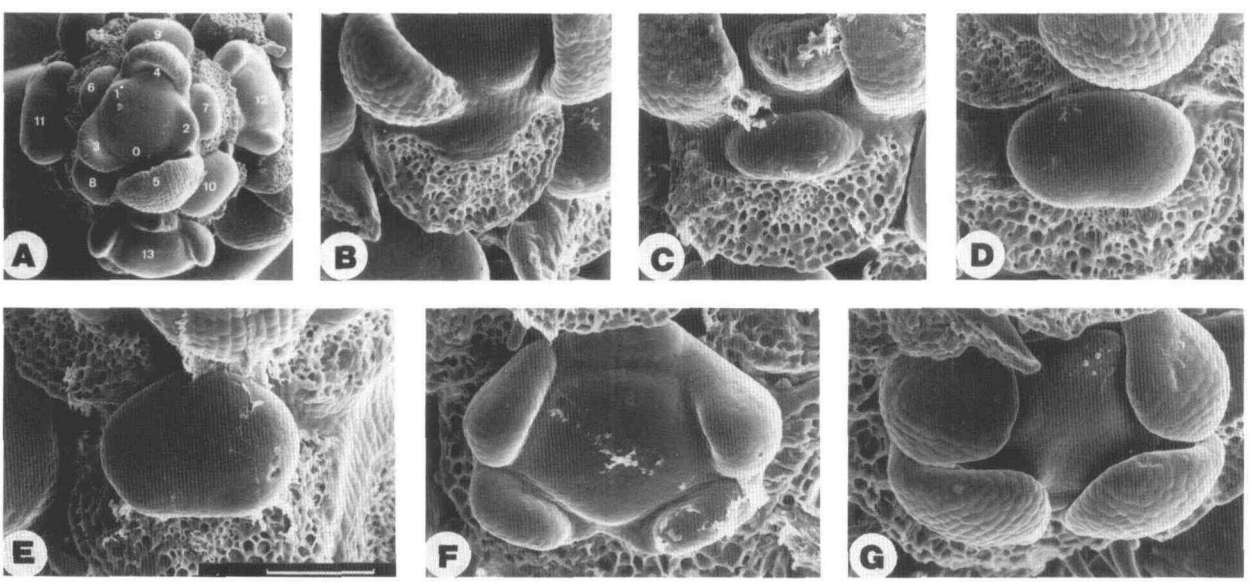

Figure 1. Scanning Electron Microscopy of Different Stages of Wild-Type Antirrhinum.

(A) Inflorescence apex with nodes numbered sequentially (see Results for explanation).
(B) Stage 1, eye.
(C) Early stage 2, loaf.
(D) Late stage 2, loaf.
(E) Stage 3, pentagon.
(F) Stage 4, floritypic.
(G) Stage 5, petal mound.
Individual meristems are oriented with bract at the base. The DV axis is vertical, and the ML axis is horizontal. Both axes go through the center of each meristem. Bar in **(E)** = 100 μm.

cells long (50 μm) but lengthened during this stage to ~15 cells (150 μm), at which point it occupied approximately one-quarter of the circumference of the apex.

Stage 1: Eye (Nodes 4 to 8)

An eye-shaped group of cells (floral meristem) was visible between each bract primordium and the main stem (Figure 1). The bract primordia had a hooded shape and appeared to grow over and protect the axillary floral meristems. When first visible, the eye was 9 to 12 cells along the ML axis (110 μm) and 4 to 6 cells along the DV axis (20 μm); the dimensions of the cells were relatively compressed along the DV axis (10 × 5 μm). By the end of this stage, the eye had become more elliptical in shape (140 × 45 μm) and the cells were isodiametric (10 × 10 μm).

Stage 2: Loaf (Nodes 8 to 10)

The floral meristem had a nearly rectangular shape and was raised up like a loaf of bread. Toward the end of this stage, the loaf was ~160 × 110 μm. The cells in the medial region of the loaf were elongated along the DV axis (10 × 17 μm), whereas at the ends of the loaf, they were isodiametric in shape (10 × 10 μm).

Stage 3: Pentagon (Nodes 10 to 12)

The fivefold nature of the floral meristem was discernible and gave the meristem a more pentagonal shape. Toward the end of this stage, the sepal primordia had just started to become visible as small bulges, and the meristem was ~240 × 200 μm. Most cells were isodiametric in shape (10 × 10 μm).

Stage 4: Floritypic (Nodes 12 to 14)

The sepal primordia were clearly visible and separated by a crease from the rest of the floral meristem. The back (dorsal) sepal primordium appeared to be slightly retarded in its development relative to the other sepals. Toward the end of this stage, the overall dimensions of the flower were ~300 × 240 μm. The creases at the sepal bases were ~10 cells long (100 μm) and together formed an inner pentagon ~20 cells (150 μm) across. This was called the floritypic stage, because a similar morphological stage can be identified in many other species, and because it may correspond to a time by which several key developmental genes have been activated (Bradley et al., 1993).

Stage 5: Petal Mound (Nodes 15 to 18)

At the start of this stage, the sepal primordia arched over the inner pentagon of the floral meristem, the back sepal primordium being clearly smaller than the others. Five petal primordia could be seen as small mounds at the vertices of the inner pentagon. Each mound measured ~10 cells along the circumference of the inner pentagon and approximately five cells in thickness. Four stamen primordia were just visible as small undulations in the meristem in positions alternating with the petal primordia. By the end of this stage, the overall dimensions of the flower were ~450 × 320 μm. The petal primordia had adopted a tongue-like shape, and four of the stamen primordia formed rounded domes. The fifth (back) stamen primordium was retarded in its development relative to the others.

Development in *flo* and *squa* Mutants

The effects of *flo* and *squa* on development were determined by comparing the morphology of mutant meristems with those of the wild type (Figure 2). Plants homozygous for null *flo* mutations have indeterminate shoots rather than flowers growing in the axils of bracts. At the base of each of these axillary shoots is a whorl of two bracts lying opposite each other and set at right angles to the subtending bract of the main stem. The rest of the axillary shoot comprises a spiral of bracts that recapitulates the phyllotaxy of the bracts on the main stem. The *flo* mutation therefore results in reiteration of spiral phyllotaxy in axillary positions rather than the whorled phyllotaxy of the flower. The phenotype of *squa* mutants is similar to that of *flo* except that abnormal flowers are eventually produced from the axillary shoots.

The effects of two different *flo* alleles on early meristem development were analyzed. The *flo-613* allele carries the Tam3 transposon in the second exon (Coen et al., 1990). The *flo-640* allele arose from *flo-613* by imprecise excision and was shown to have an extra 8 bp (CAGACGGA) situated at the excision site by sequencing a polymerase chain reaction–amplified product. This additional sequence was not seen in the wild type. The resulting frameshift would be expected to give a truncated protein of 229 amino acids compared with 396 for the wild type.

Development of the *flo* mutants was indistinguishable from the wild type until stage 2 (loaf). During this stage, the *flo* meristem showed relatively little growth in the DV axis; the cells in the medial region of the loaf remained isodiametric rather than extending, as is seen in the wild type (Figure 2, node 9). By approximately node 11, instead of a forming a pentagon, the *flo* meristem retained a loaflike appearance, with the ends of the loaf bulging slightly. A node or so later, bract primordia were clearly seen at each end of the loaf and were separated by creases from a central meristematic area. The overall dimensions of the *flo* meristem at this stage were ~200 × 125 μm (compared with 240 × 200 μm for the wild type). By nodes 13 and 14, the two lateral bracts were hooded in shape and folded over the central meristematic area. This area had become slightly raised and had grown along the DV axis to form an oval shape. By nodes 15 and 16, bract primordia were seen emerging in a spiral phyllotaxy on the periphery of the central area, thus forming a secondary inflorescence axis. In many cases, the positions of the first three bract

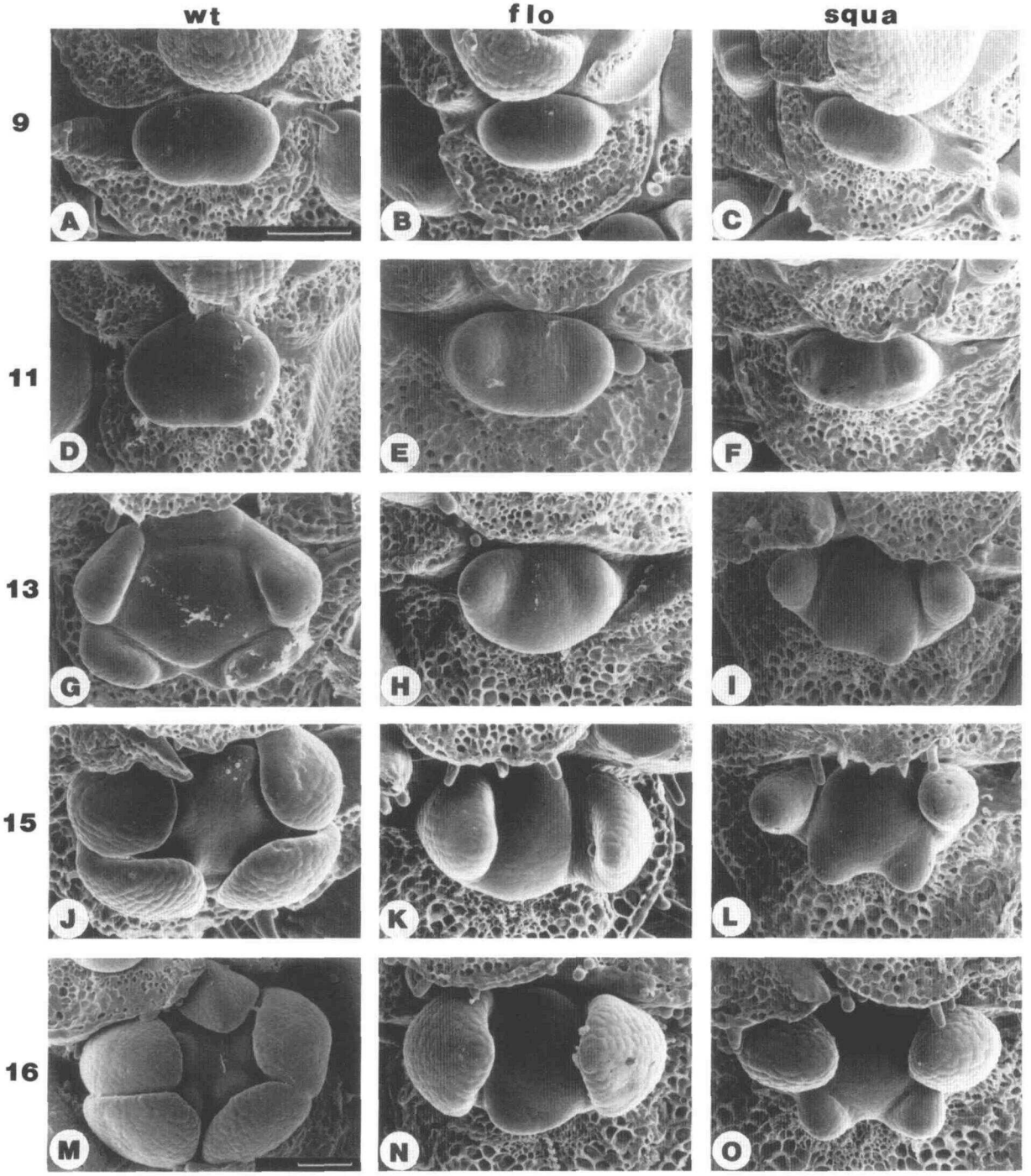

Figure 2. Comparison of Wild-Type, *flo*, and *squa* Meristems at Various Stages.

Node numbers are shown at left.

(A) to **(C)** At node 9, *flo* and *squa* inflorescence meristems show relatively little growth in the DV axis compared with wild type (stage 2).

(D) to **(F)** By node 11, the two mutants begin to show deviation from the wild-type pentagon shape (stage 3).

(G) to **(I)** Node 13 of the wild type shows floritypic (stage 4) characteristics; the sepal primordium is clearly visible. In both the *flo* and *squa* mutants, the secondary bract primordia are also visible, and there is a clear deviation in shape from both the wild type and each other.

(J) to **(L)** Shown is an early petal mound (stage 5) of the wild type as seen at node 15. By this stage, the two mutants are starting to show the development of the spiral of bracts.

(M) to **(O)** By node 16, the petal primordia are clearly visible in the wild type and the shape of the secondary bracts of the two mutants.

All of the meristems are orientated so that the subtending bract is at the base. Bar in **(A)** = 100 μm for **(A)** to **(L)**; bar in **(M)** = 100 μm for **(M)** to **(O)**.

primordia around the new axis corresponded approximately to the positions of the back sepal and two front sepals of a wild-type flower.

The effects of four different *squa* alleles were analyzed. The *squa-443* allele carries a 6-kb insertion in the first large intron of the *squa* gene and produces no detectable *squa* transcripts (Huijser et al., 1992). DNA gel blots showed that both *squa-641* and *squa-702* contained insertions in the first intron of at least 5.6 and 4.8 kb, respectively (data not shown). Polymerase chain reaction analysis showed that the *squa-701* allele contained an insertion of *Tam3* in the first intron. This allele appeared to give a weaker phenotype than the others because flowers were produced much more regularly on the inflorescence.

Development of the *squa* mutants was indistinguishable from *flo* until approximately node 14 (Figure 2). At this stage, the lateral bract primordia of *squa* meristems were rounder and less hooded than those of *flo*. In some cases, these primordia eventually developed into threadlike filamentous structures rather than bractlike organs. The central area of the meristem was raised and had two ventral primordia starting to develop, giving it an almost triangular or inverted heart shape (Figure 2, node 15). By nodes 15 and 16, the two ventral primordia formed fingerlike projections, and a crease separated them from the central meristem. An additional primordium was observed in a dorsal position, similar to the location of the back sepal primordium of a wild-type flower meristem. All alleles investigated showed a similar pattern of development.

Figure 3. Clusters of Carpels Formed on Inflorescences of Aging *flo* Mutants.

United carpels with red stylar tissue are surrounded by numerous bract or sepal-like organs. The tips of these organs sometimes bear stigmatic tissue.

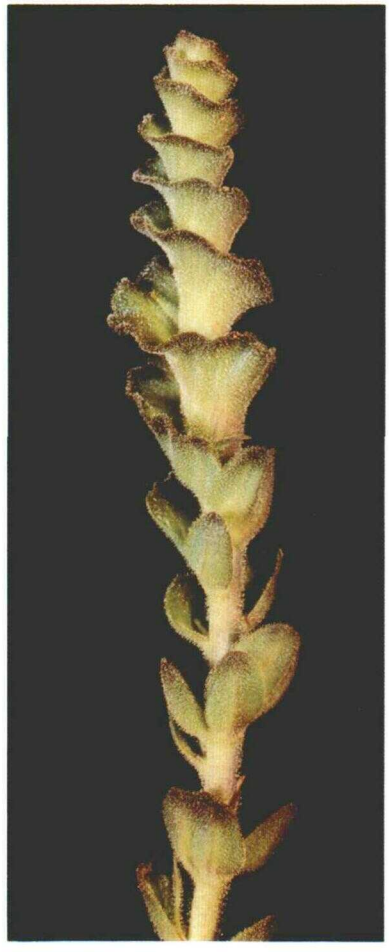

Figure 4. Double-Helical Spiral of United Bracts of a *flo* Mutant Inflorescence.

The lower part of the inflorescence shows the transition from separate to united growth.

Late Aspects of *flo* and *squa* Mutants

Plants homozygous for the *flo-640* allele continually produced inflorescence-like shoots instead of flowers and had an indeterminate growth pattern. Occasionally, however, a cluster of bracts or sepals, and carpelloid organs was observed on these plants (Figure 3). These clusters were produced from inflorescence shoots in either axillary or terminal positions. They were observed on plants toward the end of the outside growing season or on plants that had been maintained in the glasshouse for a long time.

An even rarer event seen with old *flo-613* plants was the production of continuous double helices from the apex of the inflorescence (Figure 4). The double helices were not very stable, and the inflorescence apices often reverted back to producing separate bracts. Scanning electron microscope analysis of the apex of a double helix revealed two continuous spiral

primordia originating from opposite positions on the periphery of the inflorescence apical zone (Figure 5). The spirals could be superimposed on a normal inflorescence and appeared to delineate the positions of bracts, with the sequence of bract numbers alternating between the two spirals (Figure 5). In some cases, undulations were seen along each spiral, possibly indicating a tendency for the continuous primordia to break up into separate bracts. Double spirals were also occasionally observed in scanning electron micrographs of *squa-641* apices, but their continuity was incomplete.

Genetic Interactions between *flo* and *squa*

To determine how *flo* and *squa* might interact with each other to control floral development and phyllotaxy, various double mutants were constructed. In scoring progeny from the crosses, plants were classified as flo if they did not produce any flowers having petals or stamens, or squa if they eventually produced flowers (flowers on squa plants typically have all four whorls of organs). Both *flo* and *squa* mutants were generated by crossing a line homozygous for *squa-443* to a plant heterozygous for *flo-640*. Seed obtained from selfing one of the F_1 plants from the cross were grown outside and gave an F_2 population segregating 44 wild type:33 flo:17 squa, indicating that both *flo* and *squa* were segregating.

To produce a sufficient number of plants homozygous for both *flo* and *squa*, DNA blots were first performed on the F_2 population to identify squa plants that were *flo/Flo*$^+$ heterozygotes. This was possible because the parental lines carrying the *flo* and *squa* mutations had different genetic backgrounds. The DNA from each line was therefore screened with various restriction enzymes and probed with *flo* to find a restriction fragment length polymorphism that distinguished between the *flo-640* allele (coming from the *flo* parent) and the *Flo*$^+$ allele (coming from the *squa* parent). EcoRV proved to be most useful and was used with DNA of several F_2 plants with a squa phenotype to identify several *squa/squa:Flo*$^+$*/flo-640* plants. These were self-pollinated to give progeny homozygous for *squa* but segregating for *flo*.

The progeny were grown in the glasshouse and fell into three phenotypic classes: squa, extreme squa (i.e., producing squa-type flowers but only very rarely), and flo. To test whether the difference between the squa and extreme squa phenotypes might reflect an interaction with *flo*, one family of 30 plants, comprising 10 squa, 11 extreme squa, and 9 flo, was selected for DNA analysis. All 10 squa plants were homozygous for *Flo*$^+$, whereas the 11 extreme squa plants were heterozygous for *Flo*$^+$ and *flo-640*. These results indicated that the ability of *squa* mutants to produce flowers was greatly diminished either by *flo-640* in a heterozygous state or by a factor linked to *flo-640* (i.e., the probability of all squa plants being *Flo*$^+$*/Flo*$^+$ by chance is $0.33^{10} = 0.000015$). Four of the plants with a flo phenotype were homozygous for *flo* and *squa*, indicating that *flo* was epistatic to *squa*. Scanning electron microscopy confirmed that the apices of such plants were indistinguishable from those of *flo*. However, five of the plants scored as a flo phenotype were heterozygous at *flo*. One explanation for this is that the rarity of flowers on extreme squa plants sometimes led to them being misclassified as flo. This was confirmed by scanning electron microscopy of these plants, showing that they had axillary meristems typical of *squa* mutants.

An enhancement of the squa phenotype was also observed in a cross involving the *flo-639* allele. This allele arose by imprecise excision of *Tam3* from *flo-613*, resulting in a 2-bp

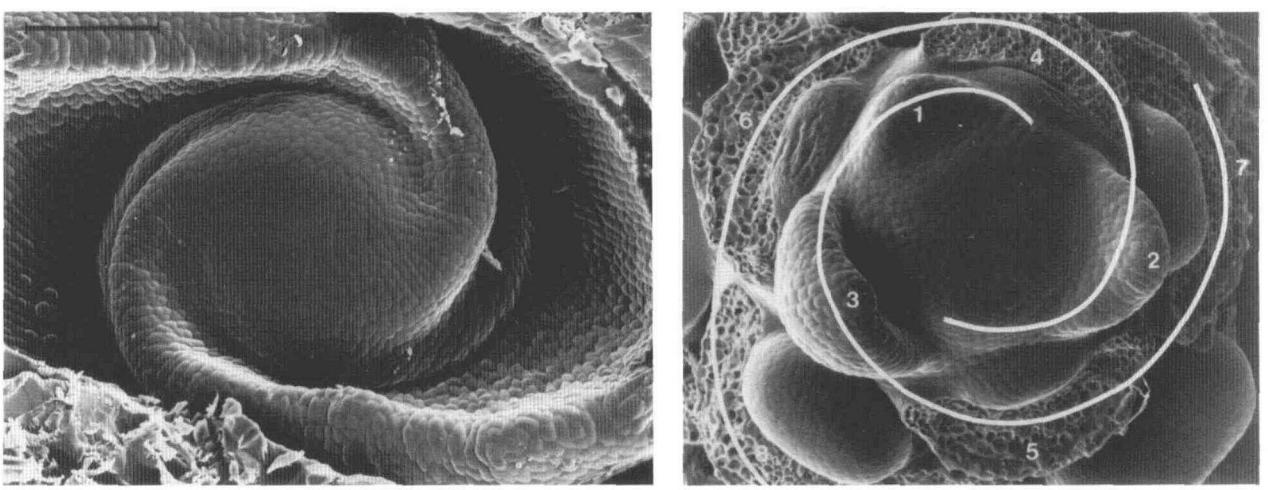

Figure 5. Apex of a *flo* Mutant Double Helix Compared with That of the Wild Type.

(Left) *flo* mutant.
(Right) Nodes of the wild type are numbered sequentially, and a double helix has been superimposed for comparison with the *flo* mutant. Bar = 100 μm.

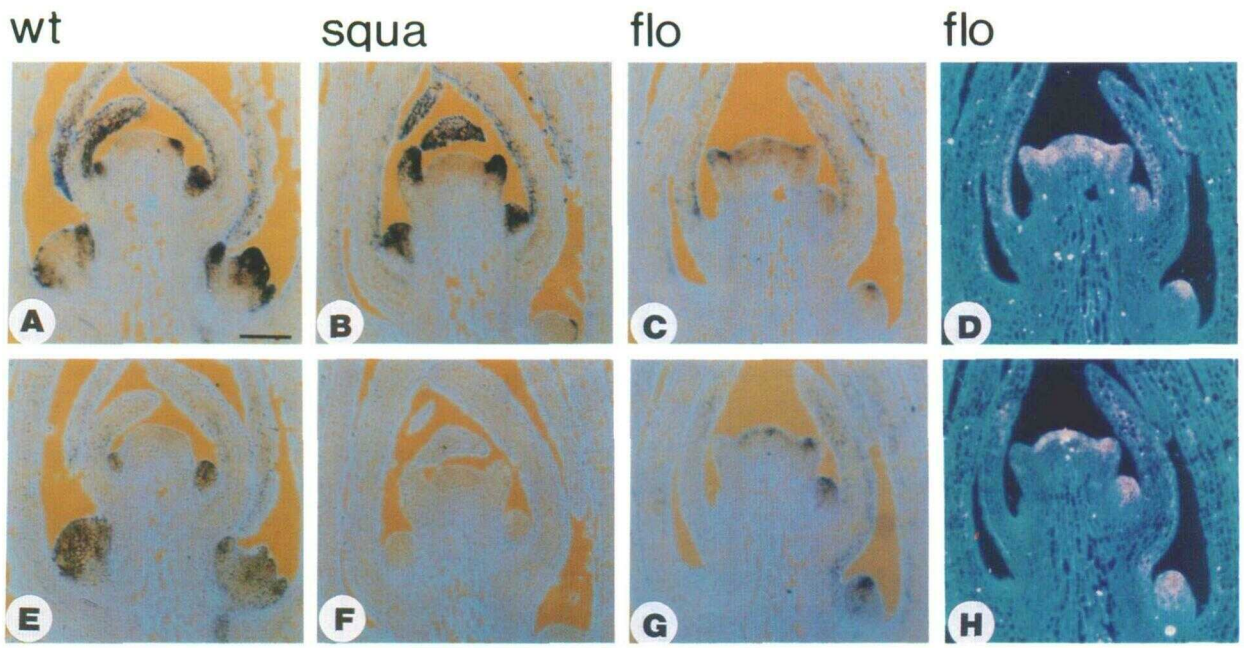

Figure 6. RNA in Situ Hybridization of Wild-Type, *squa*, and *flo* Inflorescences.

(A) to **(D)** Tissues were probed with *flo*.
(E) to **(H)** Tissues were probed with *squa*.
In **(A)** to **(C)** and **(E)** to **(G)**, the signal is dark blue on a light blue background. The weak signal in **(C)** and **(G)** is shown more clearly under dark-field illumination in **(D)** and **(H)**, respectively. Here, the signal appears pink on a turquoise background. Bar in **(A)** = 100 μm for **(A)** to **(H)**. wt, wild type.

substitution at the excision site, but gives a phenotype indistinguishable from that of the wild type (Coen et al., 1990). This footprint does not change the *flo* reading frame but gives a predicted polypeptide with a 2–amino acid substitution. *flo-639/flo-613* heterozygotes have an apparently wild-type phenotype, indicating that one dose of the *flo-639* allele is able to confer normal flower development. A plant carrying *flo-639* was crossed to a *squa-443* homozygote, and F_1 plants heterozygous at both loci were self-pollinated. The resulting F_2 progeny were grown outside and segregated 64 wild type, 18 squa, and 11 plants that appeared flo-like. DNA analysis with 10 of the flo-like plants showed that they were all homozygous for *flo-639*, whereas representatives of all three possible *flo* genotypes were found in the wild-type plants. This indicated that the squa phenotype is enhanced in a genetic background homozygous for *flo-639* (the probability of all 10 of the flo-like plants analyzed being homozygous is $0.25^{10} = 0.000001$). Alternatively, a recessive enhancer of *squa* was linked to *flo-639*.

To distinguish the effects of *flo* from those of a linked gene, an additional family segregating for *flo* and *squa* was analyzed. In this case, both alleles used in the cross, *squa-641* and *flo-640*, had been derived from the same inbred line by selfing and should therefore have had very similar genetic backgrounds. From an F_1 plant that was *squa/Squa*$^+$ and *flo/Flo*$^+$, an F_2 population was derived that segregated 55 wild type, 13 squa, and 26 flo. Of the squa plants, six had a more extreme phenotype and were shown to be heterozygous for *flo*, whereas plants with a weaker squa phenotype were homozygous for *Flo*$^+$. This confirmed that the squa phenotype is enhanced by *flo-640* in the heterozygous state.

Expression of *flo* and *squa* in Wild-Type and Mutant Backgrounds

The interactions between *flo* and *squa* were studied further by comparing their expression patterns in wild-type and mutant inflorescences. Comparisons were most meaningful up to the stage at which the morphologies of mutant and wild-type meristems start to diverge (loaf, stage 2). Consecutive longitudinal sections of inflorescence apices were probed with digoxigenin-labeled *squa* or *flo* antisense RNA. In each section, bract primordia with their axillary meristems could be seen at various developmental stages below the inflorescence apex.

In the wild type, strong *flo* expression could be seen in the bract mounds and tongues of stage 0 and in eye-shaped floral meristems as soon as they could be distinguished (Figure 6A, stage 1). By stages 3 and 4, *flo* transcripts were concentrated mainly in the sepal primordia of the axillary floral meristems. In *squa-641* mutants, expression of *flo* was similar to that of

the wild type up to stage 2 (Figure 6B, loaf). For several nodes after this, *flo* transcripts were concentrated in the initiating primordia that were destined to form bracts, bracteoles, or sepals. The pattern of *flo* expression at later stages varied according to whether axillary inflorescence meristems developed, in which case it recapitulated the expression pattern seen in the inflorescence apex, or flowers started to form, in which case expression was similar to that of the wild type. The effect of *flo* on its own expression could also be analyzed by exploiting the *flo-640* mutation, which carried an 8-bp insertion in the coding region and could therefore produce a nearly normal transcript, even though the encoded protein should be truncated. Transcripts of *flo* were observed in bract primordia and their axillary meristems in *flo-640* but were present at a much lower level than in the wild type (compare Figures 6A and 6C). Curiously, weak ectopic expression was also reproducibly observed in the inflorescence apex of *flo-640* mutants (Figures 6C and 6D).

Expression of *squa* was highest in wild-type floral meristems from stage 1 onward and was present at relatively low levels in bract primordia (Figure 6E; Huijser et al., 1992). No *squa* expression was observed in the *squa-641* mutant, as expected, because it contained a transposon insertion upstream of the region used as a probe (Figure 6F). In *flo-640*, expression of *squa* was at a level similar to that observed in the wild type (compare Figures 6E and 6G) . Ectopic *squa* expression was reproducibly observed in the inflorescence apex of *flo-640*, particularly in the outer two cell layers of the meristem (Figures 6G and 6H).

DISCUSSION

Detailed analysis of the first 18 nodes of wild-type inflorescences allows six developmental stages to be defined: (0) tongue, (1) eye, (2) loaf, (3) pentagon, (4) floritypic, and (5) petal mound. There are no obvious differences between the inflorescences of the wild type and *flo* and *squa* mutants until the start of the loaf stage. At this stage, wild-type floral meristems are approximately three times longer along the ML axis than the DV axis. During the next few nodes, wild-type meristems grow rapidly along the DV axis and eventually achieve a nearly symmetrical pentagonal shape, with five primordia starting to emerge from the periphery. In contrast, *flo* meristems keep their rectangular loaf shape for much longer. The two poles of the loaf eventually form lateral bract primordia, and the rest of the meristem, lying between them, gives rise to a secondary inflorescence axis. The first three bract primordia of this new inflorescence axis are often located almost directly over the positions occupied by the dorsal and ventral sepal primordia of wild-type floral meristems (Figure 7). Development of *squa* mutants is intermediate between *flo* and the wild type. The mutant resembles *flo* early on, forming two lateral bract primordia, but soon after this, two ventral primordia and a dorsal

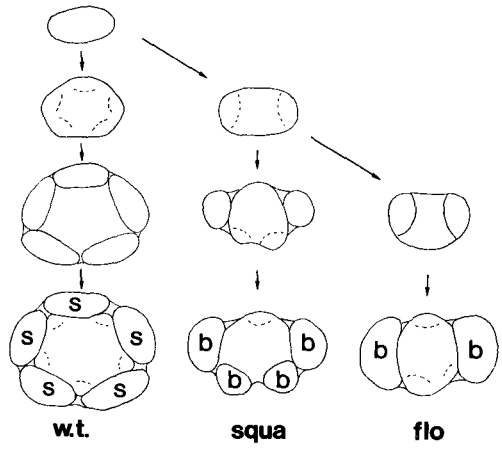

Figure 7. Comparison of Wild-Type, *squa*, and *flo* Meristem Development.

The diagram is based on scanning electron microscopy as shown in Figures 1 and 2. Dotted lines indicate regions where primordia appear to be initiating. The DV axis is vertical, and the MV axis is horizontal. Both axes go through the center of each meristem. w.t., wild type; s, sepals; b, bracts.

primordium initiate and adopt positions that are nearer to those of wild-type sepals (Figure 7). Analysis of *flo squa* double mutants confirmed that the effects of *squa* on early meristem behavior are less extreme than those of *flo*. The inflorescence apices of double mutants resemble those of *flo* rather than *squa*, indicating that *flo* is epistatic to *squa* with respect to phyllotaxy.

One way to explain these results is that the same basic mechanism of phyllotaxy underlies both wild-type and mutant meristem development but that the relative timing of primordium initiation or growth is altered. In the *flo* mutant, there is a significant delay between the initiation of the first two lateral bract primordia and the additional primordia of the secondary inflorescence axis. In the wild type, this delay is much less, resulting in three additional primordia becoming incorporated in the first whorl. This would give a total of five primordial initiating regions in the first whorl, and further interactions between them could establish the precise pentagonal symmetry of the flower. This could explain why the bract primordia of secondary *flo* inflorescences are often positioned at angles around the axis similar to those of the sepal primordia of a flower meristem. The intermediate development of *squa* mutants can also be explained if their delay in primordium initiation is greater than the wild type but less than *flo*. These effects on timing might reflect the normal action of *flo* and *squa* in accelerating the initiation of primordia just before the loaf stage of the wild type (i.e., before the primordia are visible as outgrowths). This would result in extra primordia occupying dorsal and ventral positions, accounting for the rapid growth in the DV axis observed during the loaf stage. Alternatively, the genes

could first act to increase growth along the DV axis, and this could then provide additional space to allow extra primordia to initiate.

The *flo* and *squa* genes interact with each other to control flower development. Reduction of *flo* activity to levels that would normally have no effect on floral development can greatly enhance the *squa* mutant phenotype, leading to a delay or prevention of flower production. The interactions between *flo* and *squa* do not seem to operate directly at the transcriptional level. Early expression patterns of *flo* and *squa* in axillary meristems are not influenced by *squa* and *flo* mutations, respectively. These results show that *flo* and *squa* are initially switched on independently of each other, but once activated, they interact to promote floral development. Additional evidence for independent pathways comes from the observation of clusters of carpelloid organs on old *flo-640* plants. This suggests that some aspects of floral development may eventually be activated by a *flo*-independent pathway, possibly involving the *squa* gene. However, petals and stamens have never been observed in *flo-640* mutants, indicating that these organ types have an obligatory requirement for Flo^+ activity for their development.

Although the level of *flo* transcription does not appear to be strongly affected by *squa* mutations, it is markedly reduced in *flo-640* mutants, which carry a frameshift in the middle of the *flo* coding region. This suggests that *flo* normally increases its own expression through autoregulation so that in *flo* mutants, expression fails to increase beyond a basal level. High levels of *flo* expression might therefore be established only in meristems initially having a critical level of *flo* activity, possibly helping to ensure that switches between shoot and flower meristem identities are discrete and intermediate states are not favored.

In addition to having reduced *flo* expression in axillary meristems, *flo-640* mutants show ectopic *flo* and *squa* expression in the inflorescence apex. This indicates that Flo^+ activity in bracts or floral meristems may act nonautonomously to prevent expression of *flo* and *squa* in the apex. Alternatively, Flo^+ activity may initially be present in the apex but then rapidly inhibits its own expression and that of *squa*. The expression of genes, such as *squa*, in the inflorescence apex may have some functional significance because clusters of carpelloid organs are occasionally seen at terminal positions on inflorescences of *flo-640* mutants, suggesting that the apex of *flo* mutants has aquired some floral characteristics.

The observations on the interactions of *flo* and *squa* have many parallels with the homologous mutations in Arabidopsis *leafy* (*lfy*) and *apetala1* (*ap1*), respectively (Huala and Sussex, 1992; Mandel et al., 1992; Weigel et al., 1992; Bowman et al., 1993; Schultz and Haughn, 1993). For comparison, it is useful to describe the lfy phenotype in terms of an early phase, in which shoots replace flowers, and a late phase, in which clusters of sepals and carpels replace flowers. The early *lfy* phase is very similar to that of *flo*, whereas the late phase is similar to the rare carpelloid clusters seen with old *flo* plants. With respect to initial phyllotaxy, *lfy* is epistatic to *ap1* in the early phase, but the late phase is delayed in *lfy ap1* double mutants. As with *flo* and *squa*, transcript levels of *lfy* appear to be established independently of *ap1* in young floral meristems. However, unlike *flo*, there is no evidence for autoregulation of *lfy*. This may be because the analysis of expression in *lfy* mutants was performed on meristems in the late rather than early phase. Perhaps, *lfy* expression can be maintained by other genes during the later phases, making autoregulation redundant. It is also possible to explain the effects of *lfy* on phyllotaxy by a model similar to that invoked for *flo*. During the early phase, a *lfy* meristem first initiates a primary bract (cauline leaf) primordium; after a delay, this is followed by the initiation of further bract primordia on the secondary inflorescence axis. If the delay between the initiation of the primary bract and the following three bracts were greatly reduced, it would give a total of four initiating primordia in the first whorl in positions that might anticipate the cruciform symmetry of the wild-type flower. Further interactions between these four initiating regions could ensure that the precise symmetry of the flower is established. This is consistent with the view that the bracts of *lfy* mutants derive from a region that would normally give rise to part of the flower (Weigel et al., 1992; Coen and Carpenter, 1993).

Further insights into the possible mechanism underlying phyllotaxy come from the observation of double helices occasionally found in old *flo* mutant plants. These are generated by a continuous double spiral at the inflorescence apex. If the two arms of the spiral are superimposed over the wild type, all underlying bract primordia can be accounted for, with consecutive bract primordia alternating between the two spirals. This shows that setting aside zones for primordium initiation and partitioning these zones into discrete primordia are separable events. The formation of continuous primordia has also been observed in mutants causing fasciation, but in these cases meristem size and structure are more profoundly disrupted (Leyser and Furner, 1992; Clark et al., 1993). One explanation for the double helix phenotype is that initially, distinct bract primordium-forming regions unite at a very early stage with their nearest neighbors to form continuous spirals. This is consistent with most models of phyllotaxy, which postulate that primordia are initiated discretely. Alternatively, the continuous spirals may reflect the primary state, and in wild-type meristems the continuity is broken up and partitioned to form discrete primordia. According to this view, two primordial initiation zones at opposite positions may continually rotate around the apex of the inflorescence, each taking ~4 days to make a full circuit in Antirrhinum (each spiral makes approximately one node per day at a divergence angle of ~85°). Such a view is reminiscent of theories of Plantefol, who postulated a series of primary helices underlying all types of phyllotaxy (Plantefol, 1948; Loiseau, 1969).

Whichever model is correct, the observation of double helices on *flo* mutants suggests that *flo* may play a role in partitioning of the apical meristem. Clearly, Flo^+ activity is not absolutely required for partitioning because most *flo* mutant

inflorescences produce discrete bracts. Nevertheless, expression of *flo* in defined regions of the apex may help to establish distinctions between nearby groups of cells.

METHODS

Plant Material and Scanning Electron Microscopy

Plants (*Antirrhinum majus*) were grown under the conditions laid out in Carpenter et al. (1987). The *floricaula* mutant *flo-613* was obtained from a large-scale transposon mutagenesis program performed at the John Innes Institute as described in Carpenter and Coen (1990). The mutants *flo-639* and *flo-640* were both derived from the self-pollination of flowering sectors produced by *flo-613* (Coen et al., 1990). During the transposon mutagenesis program, the *squamosa* mutant *squa-641* was derived from stock JI 523, itself a revertant of the JI 98 line (Sommer et al., 1985; Carpenter et al., 1987). The *squa-702* mutant was derived from a heterozygote of a semidominant *nivea* mutation, *niv-527* (Bollmann et al., 1991) and wild-type Antirrhinum (stock JI 7). Seed of the *squa-443* was obtained from P. Huijser (Max Planck Institut für Züchtungsforschung, Cologne, Germany) and came originally from the Gatersleben Collection (Baur, 1930; Huijser et al., 1992).

Scanning electron micrographs were prepared according to the method described by Green and Linstead (1990). The floral nodes were numbered sequentially, starting from the apex of the meristem and working down the inflorescence.

In Situ Hybridization and DNA Analysis

Methods for digoxigenin labeling of RNA probes and in situ hybridization were as described by Bradley et al. (1993), as was the template for the *flo* probe. The *squa* probe template consisted of an EcoRI fragment containing the complete cDNA with the poly(A) tail removed; it was supplied in pBluescript vector KS+ by P. Huijser (clone pBDef H33.1) and was linearized with BamHI, which removes the MADS box. The sense control probe was obtained by subcloning the cDNA insert into pBluescript vector KS+. The methods for DNA extraction and DNA blot analysis were as described previously (Coen et al., 1986; Coen and Carpenter, 1988). Polymerase chain reaction amplification and sequencing were performed according to Hantke et al. (1995) using oligonucleotides 1 (5′-TGCCATCAATTGCATGCATGAAA-3′) and 2 (5′-GCAAGCTTGCTCGTACAAATGAAACA-3′). The resulting amplification product was sequenced using the double-stranded DNA cycle sequencing system from Bethesda Research Laboratory according to the manufacturer's instructions using oligonucleotides 3 (5′-GGTTGTCGGAGGAGCCGGTGC-3′) and 2 (as given above). The near wild-type allele used in the crosses with *squa* was sequenced in the same way and found to be identical to *flo-639* (Coen et al., 1990).

ACKNOWLEDGMENTS

We thank Peter Huijser for providing the clone of *squa* and Paul Green for help with scanning electron micrograph techniques. Helpful comments were provided by Desmond Bradley, Elizabeth Schultz, Pilar Cubas, and Gwyneth Ingram. We also acknowledge support from the Biotechnology and Biological Sciences Research Council's Plant Molecular Biology II Programme.

Received April 24, 1995; accepted September 12, 1995.

REFERENCES

Baur, E. (1930). Mutations-Auslösung bei *Antirrhinum majus*. Z. Bot. **23,** 676–702.

Bollmann, J., Carpenter, R., and Coen, E.S. (1991). Allelic interactions at the *nivea* locus of Antirrhinum. Plant Cell **3,** 1327–1336.

Bowman, J.L., Alvarez, J., Weigel, D., Meyerowitz, E.M., and Smyth, D.R. (1993). Control of flower development in *Arabidopsis thaliana* by *APETALA1* and interacting genes. Development **119,** 721–743.

Bradley, D., Carpenter, R., Sommer, H., Hartley, N., and Coen, E.S. (1993). Complementary floral homeotic phenotypes result from opposite orientations of a transposon at the *plena* locus of Antirrhinum. Cell **72,** 85–95.

Callos, J.D., and Medford, J.I. (1994). Organ positions and pattern formation in the shoot apex. Plant J. **6,** 1–7.

Carpenter, R., and Coen, E.S. (1990). Floral homeotic mutations produced by transposon-mutagenesis in *Antirrhinum majus*. Genes Dev. **4,** 1483–1493.

Carpenter, R., Martin, C., and Coen, E.S. (1987). Comparison of genetic behaviour of the transposable element Tam3 at two unlinked pigment loci in *Antirrhinum majus*. Mol. Gen. Genet. **207,** 82–89.

Clark, S.E., Running, M.P., and Meyerowitz, E.M. (1993). *CLAVATA1*, a regulator of meristem and floral development in *Arabidopsis*. Development **119,** 397–418.

Coen, E.S., and Carpenter, R. (1988). A semi dominant allele *niv525* acts in *trans* to inhibit expression of its wild-type homologue. EMBO J. **7,** 877–883.

Coen, E.S., and Carpenter, R. (1993). The metamorphosis of flowers. Plant Cell **5,** 1175–1181.

Coen, E.S., Carpenter, R., and Martin, C. (1986). Transposable elements generate novel spatial patterns of gene expression in Antirrhinum majus. Cell **47,** 285–296.

Coen, E.S., Romero, J.M., Doyle, S., Elliott, R., Murphy, G., and Carpenter, R. (1990). *floricaula*: A homeotic gene required for flower development in Antirrhinum majus. Cell **63,** 1311–1322.

Green, P.B. (1992). Pattern formation in shoots: A likely role for minimal energy configurations of the tunica. Int. J. Plant Sci. **153,** S59–S75.

Green, P.B., and Linstead, P. (1990). A procedure for SEM of complex shoot structures applied to the inflorescence of snapdragon (*Antirrhinum*). Protoplasma **158,** 33–38.

Hantke, S., Carpenter, R., and Coen, E.S. (1995). Expression of *floricaula* in single cell layers of periclinal chimeras activates downstream homeotic genes in all layers of floral meristems. Development **121,** 27–35.

Huala, E., and Sussex, I.M. (1992). *LEAFY* interacts with floral homeotic genes to regulate Arabidopsis floral development. Plant Cell **4,** 901–913.

Huijser, P., Klein, J., Lonnig, W.E., Meijer, H., Saedler, H., and Sommer, H. (1992). Bracteomania, an inflorescence anomaly, is

caused by the loss of function of the MADS-box gene *squamosa* in *Antirrhinum majus*. EMBO J. **11**, 1239–1250.

Leyser, H.M.O., and Furner, I.J. (1992). Characterization of three shoot apical meristem mutants of *Arabidopsis thaliana*. Development **116**, 397–403.

Loiseau, J.-E. (1969). La Phyllotaxie. (Paris: Masson et Cie).

Mandel, M.A., Bowman, J.L., Kempin, S.A., Ma, H., Meyerowitz, E.M., and Yanofsky, M.F. (1992). Manipulation of flower structure in transgenic tobacco. Cell **71**, 133–143.

Marc, J., and Hackett, W.P. (1991). Gibberellin-induced reorganisation of spatial relationships of emerging leaf primordia at the shoot apical meristem in *Hedera helix* L. Planta **185**, 171–178.

Mitchison, G.J. (1977). Phyllotaxis and the fibonacci series. Science **196**, 270–275.

Plantefol, L. (1948). La Theorie des Helices Foliaires Multiples. (Paris: Masson and Cie).

Richter, P.H., and Schranner, R. (1978). Leaf arrangement: Geometry, morphogenesis and classification. Naturwissenschaften **65**, 319–327.

Schultz, E.A., and Haughn, G.W. (1991). *LEAFY*, a homeotic gene that regulates inflorescence development in Arabidopsis. Plant Cell **3**, 771–781.

Schultz, E.A., and Haughn, G.W. (1993). Genetic analysis of the floral initiation process (FLIP) in *Arabidopsis*. Development **119**, 745–765.

Smyth, D.R., Bowman J.L., and Meyerowitz, E.M. (1990). Early flower development in *Arabidopsis*. Plant Cell **2**, 755–767.

Sommer, H., Carpenter, R., Harrison, B.J., and Saedler, H. (1985). The transposable element Tam3 of *Antirrhinum majus* generates a novel type of sequence alteration upon excision. Mol. Gen. Genet. **199**, 225–231.

Weigel, D., Alvarez, J., Smyth, D.R., Yanofsky, M.F., and Meyerowitz, E.M. (1992). *LEAFY* controls floral meristem identity in Arabidopsis. Cell **69**, 843–859.